Structure–property relationship of shape memory polyurethane cross-linked by a polyethyleneglycol spacer between polyurethane chains

Byoung Chul Chun · Tae Keun Cho · Mi Hwa Chong · Yong-Chan Chung

Abstract Shape memory polyurethane (SMPU) cross-linked by a polyethyleneglycol (PEG) spacer at its side was compared with a linear SMPU and the one randomly cross-linked by glycerol. The SMPU was composed of 4,4′-methylenebis(phenylisocyanate) (MDI), polytetramethyleneglycol-2000 (PTMG-2000), 1,4-butanediol (BD), glycerol, and PEG-200 as a spacer. PEG-200 connected the glycerol hydroxyl groups of two polyurethane chains via the connecting agent, MDI. T_m of the soft segment increased with the increase of cross-linking content. Cross-link density measured by the swelling experiment increased in proportion to the glycerol content. A surprising increase in maximum stress compared to the linear SMPU was attained without any sacrifice in strain. Remarkably, the stress–strain curve revealed that the PEG cross-linked SMPU exhibited a similar behavior and superior tensile mechanical properties to natural rubber. Storage modulus also increased and loss tangent became broad in distribution over the temperature range after PEG cross-linking. Shape recovery rate went up to 96.8%, and shape recovery speed was three times faster than that of linear SMPU.

B. C. Chun (✉) · T. K. Cho · M. H. Chong
Department of Polymer Engineering, The University of Suwon, Hwasung-shi, Kyonggi-do 445-743, Korea
e-mail: bcchun@suwon.ac.kr

B. C. Chun · T. K. Cho · M. H. Chong · Y.-C. Chung
Intelligent Textile System Research Center, Seoul, Korea

Y.-C. Chung
Department of Chemistry, The University of Suwon, Hwasung-shi, Kyonggi-do 445-743, Korea

Introduction

Shape memory polymer has drawn widespread attention because of the features like low density (1000–1300 kg/m^3), high shape recovery, low manufacturing cost, and ease of processing [1–4]. The first shape memory polymer, polynorborene, was introduced by Nippon Zeon company in 1984, and various forms of shape memory polymers such as poly(isoprene-butadiene-styrene), polyurethane, and polystyrene series have followed [5–8]. Among these candidates, shape memory polyurethane (SMPU), first developed by Mitsubishi Chemical in 1988, was most favored due to its excellent properties which include a wide shape recovery temperature range (–30 to 70 °C), a high shape recovery rate, easy processing conditions, and a possible biocompatibility [7, 9–11]. Like other shape memory polymers, SMPU also has a phase-separated structure where hard and soft domains are formed due to the difference in intermolecular attraction of hard and soft segments. Hydrogen bonding together with dipole-dipole interaction binds hard segments to form a hard domain which plays an important role in recovering the original shape above T_m. The flexible soft segment absorbs any external stress or impact and keeps the polymer resilient at low temperature.

Because the previous linear SMPUs are not able to withstand the cyclic distortion and recovery test, cross-linking of polyurethane has been tried by us and other researchers [4, 12, 13]. Although the addition of a cross-linking agent into the polyurethane chain improved the mechanical and shape memory properties, retention of high shape recovery rate after repetitive test cycles and attainment of higher mechanical properties remain to be resolved. Therefore, a different cross-linking method needs to be devised to improve both mechanical and shape memory properties. In our design, some of the chain

extenders, 1,4-butanediol, are replaced with glycerol that is used as a connecting spot with other polyurethane chains. The target polyurethane has a network-structure compared to the randomly cross-linked one, and a substantial improvement in mechanical and shape memory properties is achieved. In this investigation, PEG-200 is selected as the spacer because of its flexibility and short chain length, and the mechanical and shape memory properties are compared with linear or randomly cross-linked ones.

Experimental

Materials

4,4′-methylenebis(phenylisocyanate) (MDI, Tokyo Kasei), poly(tetramethyleneglycol) (PTMG, Aldrich Chemical, Mw = 2 kg/mol), and polyethyleneglycol (PEG-200, M_w = 0.2 kg/mol, Duksan Chemical) were dried under high vacuum (0.1 mmHg) for 432,000 s before use. 1,4-butanediol (BD, Duksan Chemical) and glycerol (Duksan Chemical) were also dried under high vacuum. Dimethylformamide and phthalic anhydride were also obtained from Duksan Chemical.

Polymer synthesis

In a 5×10^{-4} m³ four neck cylindrical flask, a mixture of MDI and PTMG was allowed to react by mechanical stirring under nitrogen purge at 50 °C for 7200 s to prepare the prepolymer. After the addition of BD and glycerol dissolved in 3×10^{-5} m³ of dry DMF to the prepolymer, the reactants were stirred under the same conditions for another 3600 s. The final PU product was dried at 60 °C for 144,000 s to remove the DMF. The amount of each reactant is shown in Table 1, where the hard segment content is fixed at 30 wt%. Synthesis of the C1 series finished at this step, but the C2 series continued for PEG cross-linking. In the C1 series, glycerol can randomly cross-link PU chains, but PEG-200 in the C2 series cross-links PU chains through glycerol hydroxyl groups. The hydroxyl number was measured to determine the molarity of free hydroxyl group on the prepolymer by a titration method shown in the following section. An exact amount of MDI based on the hydroxyl number was added to the prepolymer solution and the reaction mixture was stirred under the same conditions for 3600 s. Subsequently, PEG-200 equivalent to half mole of MDI was added, and the mixture was stirred under the same conditions for 3600 s. The C2 series product was dried at 60 °C for 144,000 s to remove DMF. As a control, linear PU without glycerol was prepared for comparison. The SMPU structures are shown in Fig. 1. A specimen was prepared for mechanical testing

Table 1 Composition of linear and cross-linked SMPU

Sample code	Reactant, mol ratio					wt.% of glycerol
	MDI	PTMG	BD	Glycerol	PEG-200	
L-0	5.0	2.0	3.0	–	–	–
C1-5	5.0	2.0	2.775	0.15	–	5
C1-10	5.0	2.0	2.55	0.3	–	10
C1-15	5.0	2.0	2.325	0.45	–	15
C2-5	5.0	2.0	2.85	0.15	0.15	5
C2-10	5.0	2.0	2.7	0.3	0.3	10
C2-15	5.0	2.0	2.55	0.45	0.45	15
C2-20	5.0	2.0	2.4	0.6	0.6	20
C2-25	5.0	2.0	2.25	0.75	0.75	25

by the solvent-casting method: DMF in the PU solution was slowly evaporated at 70 °C for 216,000 s to yield a 7×10^{-3}–9×10^{-3} m thick PU sheet and the specimen was prepared from that sheet according to ASTM D638.

Number of hydroxyl groups

The number of free hydroxyl group in the PU chain after glycerol insertion was found by following the titration method [14]. Phthalic anhydride solution was prepared by dissolving 0.014 kg of phthalic anhydride in 9.15×10^{-5} m³ of DMF. Phthalic anhydride solution (5×10^{-6} m³) was added to 2×10^{-6} m³ of the PU reaction mixture, and the mixture was sonicated for 600 s at 45 °C, incubated at 98 °C for 900 s, and allowed to cool to room temperature. After the addition of 1×10^{-5} m³ of DMF and 2×10^{-6} m³ of distilled water, the mixture was titrated with 0.1 N NaOH using a drop of 1% phenolphthalein indicator. Blank titration of the phthalic anhydride solution was carried out without the reaction mixture by the same procedure. An average of five titrations was used for the hydroxyl number calculation. The exact mass of PU in a sampled reaction mixture was found by weighing the residue after complete evaporation of DMF in a vacuum oven for 108,000 s. The hydroxyl number was calculated from the following equations.

$$0.1(B - A)/\text{PU mass} = \text{Hydroxyl number} \quad \text{(mol/kg)} \quad (1)$$
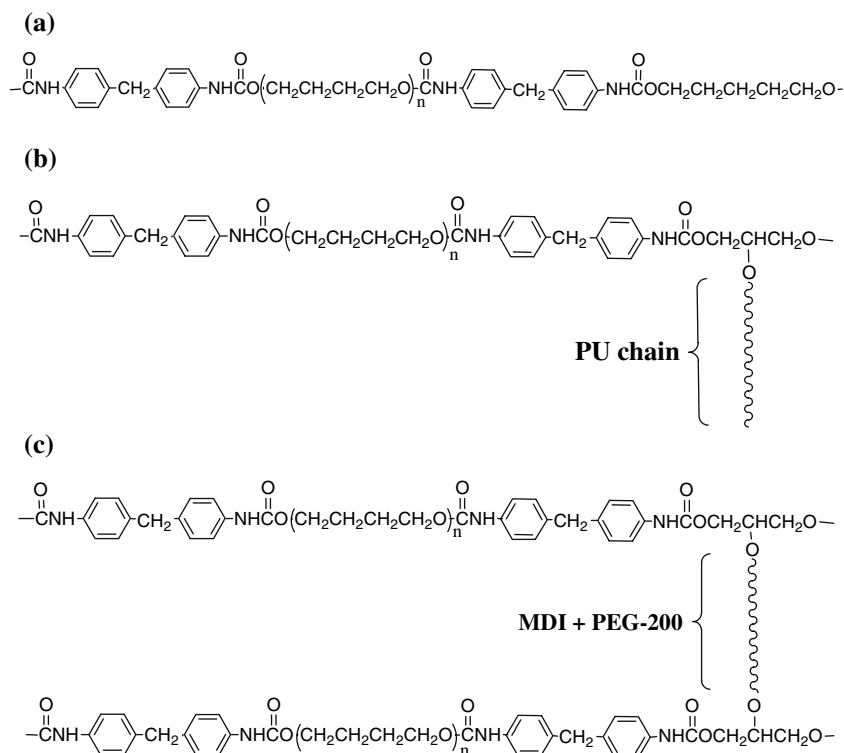
(A = titration volume of PU, and B = blank volume)

$$\text{Hydroxyl number} \times \text{Total mass} = \text{Total hydroxyl group} \quad (2)$$

Characterization

A FT-IR spectrometer (JASCO 300E) equipped with ATR was used to take an IR spectrum of the PU sample with

Fig. 1 Structures of (**a**) L-0,
(**b**) C1 series, and (**c**) C2 series

(a)

(b)

PU chain

(c)

MDI + PEG-200

400 m^{-1} resolution, 25 scans, and a scan speed of 2×10^{-3} m/s. X-ray diffraction spectra were scanned under the conditions of $2\theta = 5°–40°$ and 0.016°/second by a wide-angle X-ray diffractormeter (WAXD, Rigaku Rint 2000, CuKα, 40,000 V, and 0.03 A). A differential scanning calorimeter (DSC-2010, TA instrument) was used for the heating and cooling scan at a rate of 0.16 °C/s between –100 °C and 250 °C. The tensile mechanical properties were measured by a Universal Testing Machine (LR50K, Lloyd instrument, UK) according to ASTM D638 using 0.025 m gauge length, 1.6×10^{-5} m/s crosshead speed, and a 2500 N load cell. The dynamic mechanical properties were measured by a dynamic mechanical analyzer (DMA-2980, TA instrument). The storage modulus and loss tangent (tan δ) were scanned between –80 °C and 65 °C at a heating rate of 0.05 °C/s, and 1 Hz. The cross-link density was calculated according to the Flory–Rehner equation for a specimen ($0.025 \times 0.025 \times 0.001$ m) swelled in toluene, a process for which further explanation will appear in the results section.

Shape memory test

The UTM was also used for the cyclic shape memory test. L_o was the original length of the specimen. The shape retention rate was calculated by Eq. (3). L_1 was measured after the specimen had been drawn 100% at 20 °C above the T_m of the soft segment for 300 s, and then allowed to

shrink at 20 °C below the T_m for 1800 s. The shape recovery rate was calculated by Eq. (4). L_2 was measured after the stretched specimen had been incubated at 20 °C above the T_m for 600 s and cooled at 20 °C below the T_m. The shape memory test was repeated three times.

$$\text{Shape retention rate} = (L_1 - L_o) \times 100/L_o (\%) \quad (3)$$

$$\text{Shape recovery rate} = (2L_o - L_2) \times 100/L_o (\%) \quad (4)$$

Results and discussion

Synthesis

Previously, the cross-linking method was dependent on the three-way linker that connected PU chains in a random manner. Connection of the nearby PU chains by a flexible cross-linker and control of the cross-link density may improve the mechanical and shape memory properties due to the resultant network structure. In this investigation, some of BD, a chain-extender, is replaced with glycerol and the extra hydroxyl group of glycerol is used as the cross-linking point. The extra hydroxyl group is activated by MDI, and PEG-200 reacts with the MDI moiety on each chain. Because a PU chain is connected side by side at the various sites along the PU chain, the overall strength can be

increased in comparison to that of the randomly cross-linked one. The free hydroxyl groups on a PU chain are found by titration method and used for the calculation of the required quantities of MDI and PEG-200 for cross-linking.

The free hydroxyl groups attack phthalic anhydride to form a polymer-phthalic acid intermediate and the excess phthalic anhydride is hydrolyzed with water to give phthalic acid (Fig. 2). The carboxyl groups from phthalic acid are titrated with the NaOH solution and the difference between the blank and the PU titration is used for the calculation of free hydroxyl groups [14]. The hydrolysis of phthalic anhydride finishes in 120 s, judging from the fact that the volume of NaOH was almost constant after 120 s (Fig. 3(a)). An aliquot of the reaction mixture after glycerol addition is taken from the reactor at 600 s interval, and the amount of free hydroxyl groups remaining after the glycerol addition is followed by the above titration method. As more glycerol reacts, the number of free hydroxyl groups decreases. Also, the number of carboxyl groups from the phthalic anhydride hydrolysis during titration increases due to the decrease in free hydroxyl groups. The glycerol reaction is over in 3600 s, as determined from the result that NaOH volume reaches its maximum in Fig. 3(b). The free hydroxyl group of the reaction mixture is calculated from the titration result, and the equivalent amount of MDI is added to activate the free hydroxyl groups. Lastly, PEG-200 is used to link the MDI-activated PU chains.
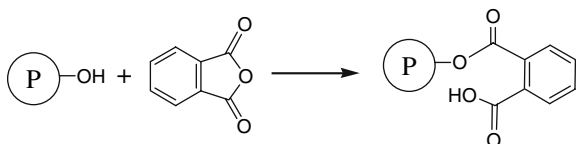

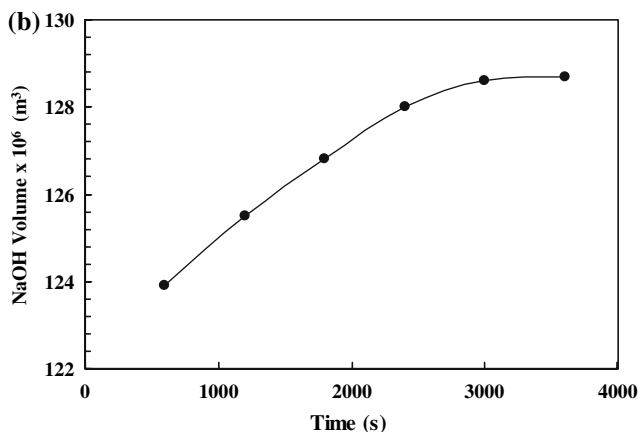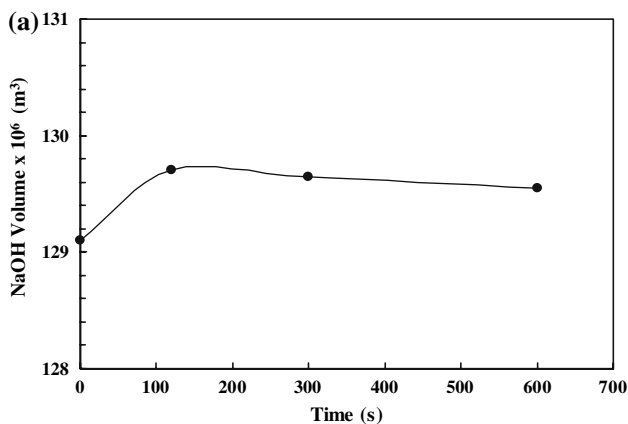
Fig. 2 Reaction between prepolymer and phthalic anhydride

Crosslink density

Cross-link density is calculated from the polymer swelling experiment. The interaction parameter (χ) between the solvent and the polymer can be found from the following Eq. (5) [15].

$$\chi = (\delta_1 - \delta_2)^2 V_1/RT \qquad (5)$$

δ_1 and δ_2 = solubility parameter of solvent and polymer; V_1 = molar volume of solvent; R = gas constant; T = absolute temperature.

Solubility parameters of toluene (δ_1) and PU (δ_2) are 18.2 and 20.5 $(MPa)^{1/2}$, respectively. The degree of cross-linking is calculated from the Flory–Rehner equation (6).

$$-[\ln(1 - v_2) + v_2 + \chi v_2^2] = V_1 n[v_2^{1/3} - 1/2v_2] \qquad (6)$$

v_2 = volume fraction of polymer in the swollen mass; χ = interaction parameter; n = cross-link density.

The cross-link density of the C1 and C2 series is summarized in Table 2. Cross-link density increases with increasing glycerol contents, and the C2 series have approximately two times higher cross-link density than the C1 series at the same glycerol content. Linear PU does not have the cross-link density. The organized cross-linking between PU chains in the C2 series has raised the cross-linking density compared to the random cross-linking of the C1 series.

IR analysis

IR peak of the hydrogen-bonded urethane carbonyl group appears at 1699–1706 cm^{-1}, a little lower than that of the free urethane carbonyl group (1731–1733 cm^{-1}) [16]. The stretching vibration of the carbonyl group is also affected by the dipole-dipole interactions between PU chains [13].

Fig. 3 (a) Time course of the phthalic anhydride hydrolysis. (b) Titration of the periodically sampled reaction mixture after glycerol addition

Table 2 Cross-link density of SMPU by swelling experiment

Sample code	ρ^a (kg/m³)	Q^b	v_2^c	$10^3 n^d$
L-0	932	–		
C1-5	999	2.620	0.276	0.547
C1-10	895	2.516	0.284	0.581
C1-15	975	2.364	0.297	0.632
C2-5	893	2.072	0.326	0.784
C2-10	934	1.832	0.353	0.954
C2-15	968	1.637	0.379	1.139
C2-20	987	1.380	0.420	1.477
C2-25	965	1.176	0.460	1.866

[a] Density; [b] Degree of swelling; [c] Volume fraction of polymer in swollen mass; [d] Cross-link density

The peak around 1730 cm⁻¹ increases slightly with the increase of glycerol content for both C1 and C2 series, while the peak around 1700 cm⁻¹ decreases (Fig. 4). Based on IR results, the shift from bonded carbonyl to free carbonyl goes on as the glycerol content increases for both C1 and C2 series. Therefore, it seems that glycerol cross-linking reduces the hydrogen bonding, and disrupts hard segment interaction.

The peak shift can be used in quantifying the phase separation of hard and soft segments. Phase separation can be also calculated from the IR spectra by comparing the peak intensity ratio of carbonyl groups at 1703 cm⁻¹ and 1733 cm⁻¹ [17]. The parameter indicating phase separation, hydrogen bonding index (R), is calculated by Eq. (7).

$$R = \frac{C_{bonded}\varepsilon_{bonded}}{C_{free}\varepsilon_{free}} = \frac{A_{1703}}{A_{1733}} \tag{7}$$

In Eq. (7), A is absorbance, C is concentration, ε_{bonded} is the extinction coefficient of the peak at 1703 cm⁻¹, and ε_{free} is the extinction coefficient of the peak at 1733 cm⁻¹.

The ratio, $\varepsilon_{bonded}/\varepsilon_{free}$, is close to 1.0 [18]. The degree of phase separation (DPS) and the degree of phase mixing (DPM) are calculated from the following equations using the R value of Eq. (7) [18]. The combined result is summarized in Table 3.

$$DPS = \frac{C_{bonded}}{C_{bonded} + C_{free}} = \frac{R}{R + 1} \tag{8}$$

$$DPM = 1 - DPS \tag{9}$$

As the glycerol content increases, R decreases from 1.15 (L-0) to 1.02 (C1-15) and 0.97 (C2-25). In the C1 series, R decreases from 1.08 (C1-5) to 1.02 (C1-15). In the C2 series, R decreases from 1.13 (C2-5) to 0.97 (C2-25). Hydrogen bonding becomes weaker as the glycerol content increases. The change in phase separation is more obvious if the DPS is compared. The DPS decreases from 53.4% (L-0) to 50.5% (C1-15) and 49.4% (C2-25). When the DPS at the same glycerol content is compared, no difference is found: 52.1% (C1-5) vs. 52.9% (C2-5), and 50.5% (C1-15) vs. 50.9% (C2-15). Now, it is clear from the IR experiment that phase separation for both C1 and C2 series is decreased by glycerol cross-linking and the difference in phase separation between them at the same glycerol content is minimal.

XRD analysis

The X-ray deflection peak of PU, irrespective of glycerol content, is observed at $2\Theta = 19.5°$ [7]. Linear PU (L-0) shows a very high peak intensity compared to cross-linked PUs, and the peak intensity decreases with any increase in glycerol content (Fig. 5). In line with the IR data, hydrogen bonding between hard segments is unaffected by cross-linking in L-0, and the ordered hard segment alignment increases the peak intensity. However, glycerol cross-linking
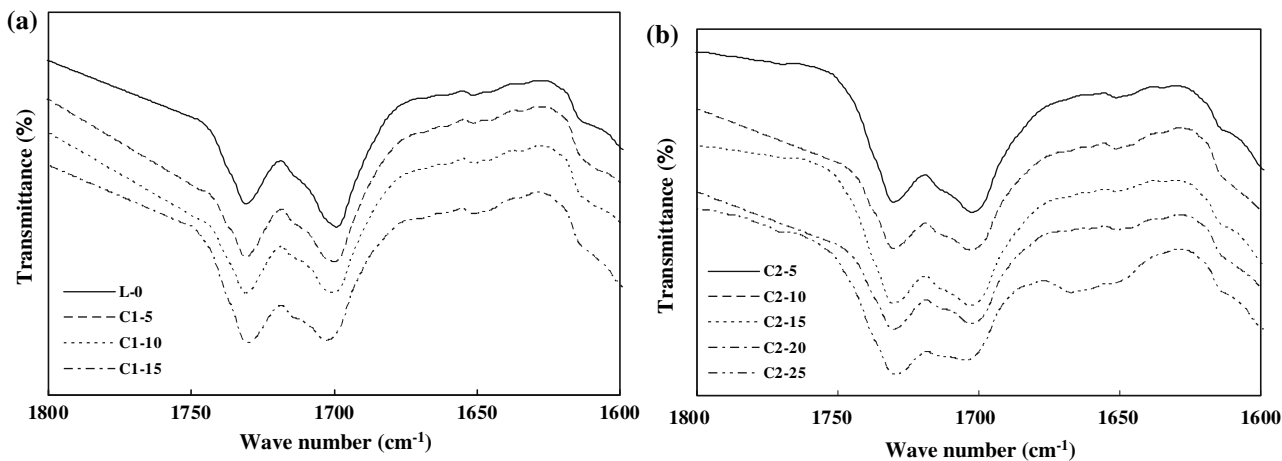

Fig. 4 Infrared spectra of (**a**) L-0 and C1 series, and (**b**) C2 series

Table 3 Comparison of thermal properties of SMPU

Sample code	R^a (A_{1703}/A_{1733})	DPS
L-0	1.15	53.4
C1-5	1.08	52.1
C1-10	1.04	51.1
C1-15	1.02	50.5
C2-5	1.13	52.9
C2-10	1.07	51.6
C2-15	1.04	50.9
C2-20	1.01	50.4
C2-25	0.97	49.4

[a] A_{1703}: absorbance at 1703 cm^{-1}, and A_{1733}: absorbance at 1733 cm^{-1}

Table 4 Degree of phase separation (DPS) and degree of phase mixing (DPM) of SMPU

Sample code	T_g (°C)	T_m (°C)	ΔH_m (J/kg)	$^a\Delta H_c$ (J/kg)
L-0	–52.47	10.00	5050	3550
C1-5	–50.72	11.35	1190	520
C1-10	–50.68	12.35	1180	110
C1-15	–49.96	11.57	1060	500
C2-5	–46.69	18.08	4040	420
C2-10	–42.99	20.35	3110	370
C2-15	–41.99	18.65	860	330
C2-20	–40.04	18.85	840	420
C2-25	–38.70	20.21	280	180

[a] ΔH_c: heat of crystallization

disrupts hydrogen bonding and hard segment alignment, and reduces the peak intensity in proportion to the glycerol content. In the extreme case of C2-25, the peak intensity is too reduced to be considered as a peak. In line with the DPS data, it is also very difficult to differentiate C1 and C2 series simply by XRD spectra.

Thermal analysis

The soft segment T_g is detected by the more sensitive DMA analysis, because it is very hard to detect T_g by DSC due to the very low temperature range and weak signal. However, it is not impossible to detect T_m of the soft segment by DSC. The combined thermal analysis data are summarized in Table 4. T_g is very low for L-0 (–52.47 °C) and increases with cross-linking for both C1 and C2 series. C2 series shows a higher T_g for a given glycerol content: –50.72 °C (C1-5) vs. –46.69 °C (C2-5) and –49.96 °C (C1-15) vs. –41.99 °C (C2-15). T_g increases up to –38.70 °C in the case of C2-25. T_m of L-0 (10.00 °C) is quite high compared to T_g and also increases with cross-linking for

both C1 and C2 series. C2 series also exhibit higher T_m at the same glycerol content: 11.35 °C (C1-5) vs. 18.08 °C (C2-5) and 11.57 °C (C1-15) vs. 18.6 °C (C2-15). Similar to the IR and XRD results, the network structure of C2 series is more influential in raising both T_g and T_m than the randomly cross-linked C1 series. It is very interesting that T_m did not increase after cross-linking although the glycerol content is raised for both C1 and C2 series. It seems that the cross-linking density of hard segment does not affect the soft segment melting because soft segment gets enough energy for melting at T_m, a relatively high temperature compared to T_g. In DSC heating scans, L-0 shows a large endothermic peak around T_m, and the endothermic peak shrinks as the glycerol content increases for both C1 and C2 series (Fig. 6). The peak area can be quantitatively compared by heat of melting (ΔH_m) in Table 4. In accordance with the peak shrinkage with cross-linking in Fig. 6, ΔH_m decreases significantly from 5050 J/kg to 1060 J/kg (C1-15) and 280 J/kg (C2-25). The restricted soft segment melting by glycerol cross-linking is responsible for the decrease of ΔH_m. The heat of crystallization
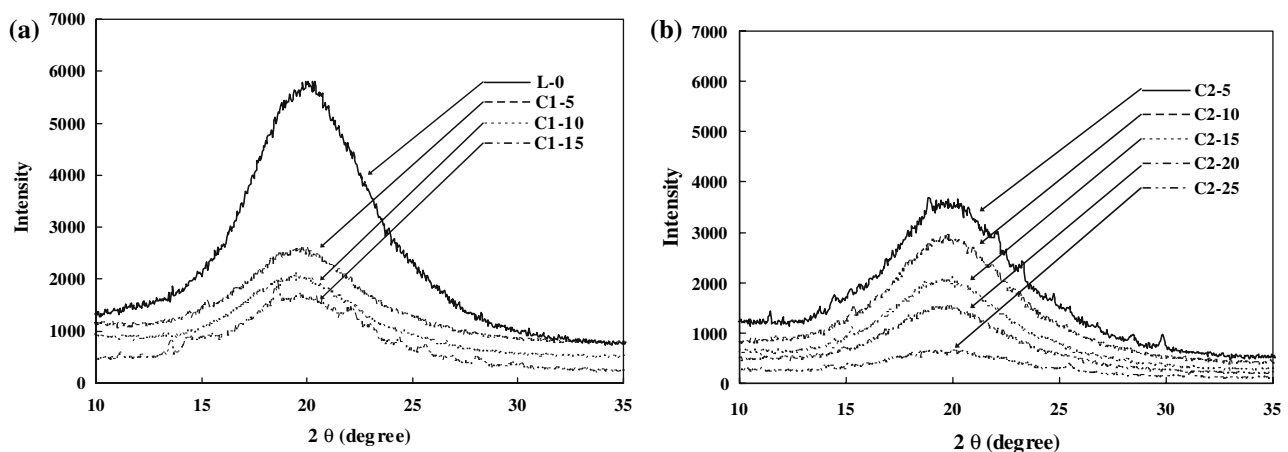
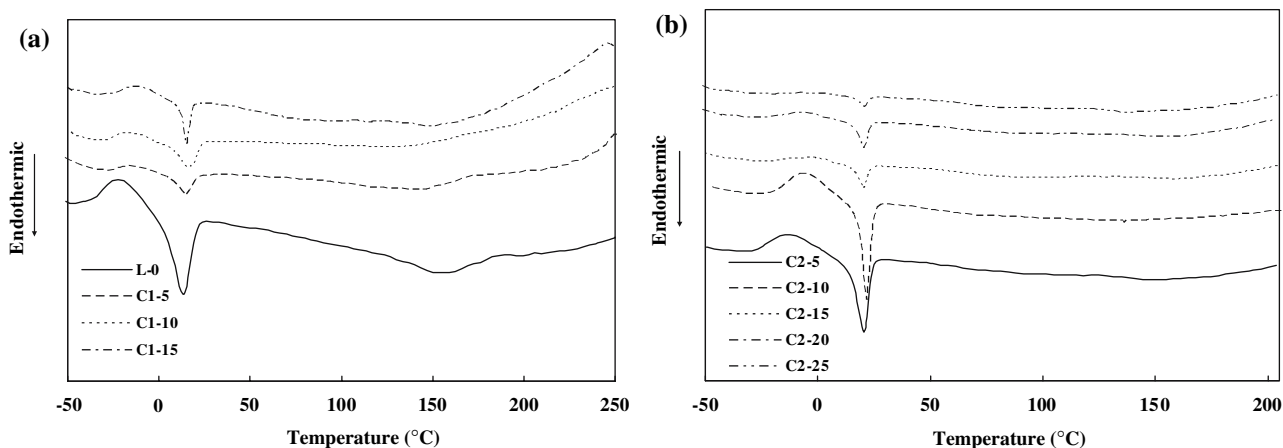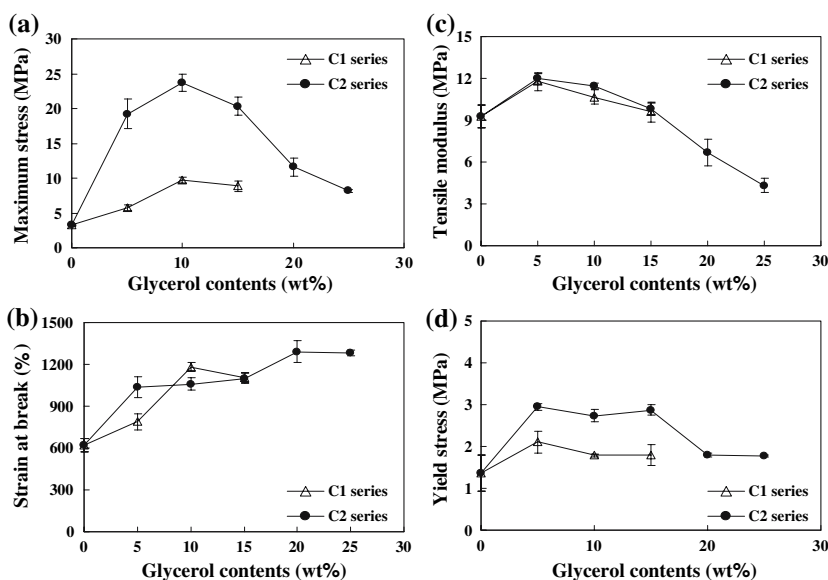**Fig. 5** X-ray diffraction spectra of (**a**) L-0 and C1 series, and (**b**) C2 series

Fig. 6 DSC heating scans of (**a**) L-0 and C1 series, and (**b**) C2 series

Fig. 7 Comparison of C1 and C2 series in the points of (**a**) maximum stress, (**b**) strain at break, (**c**) tensile modulus, and (**d**) yield stress

(ΔH_c) obtained from the cooling scan also supports that cross-linking restricts soft segment movement (Table 4).

Tensile mechanical properties

Tensile mechanical properties averaged from five tests are compared in Fig. 7. Maximum stress of cross-linked PU (C2-10) steeply increases up to 800% compared to L-0, although further increase of cross-linked content reduces the maximum stress. Maximum stress of the C2 series is 300% higher than that of C1 series at 10 wt% cross-linking. The strain at break is similar for both C1 and C2 series, and increases with the increase of cross-linking content. Tensile modulus is maximized at 5 wt% glycerol for both C1 and C2 series, and decreases with further

increase of glycerol content. Yield stress of C2 series is about 1.5 times higher than that of C1 series at 5 wt% glycerol, and decreases at higher wt% of glycerol. It is remarkable that changing the cross-linking method makes a big difference in maximum stress while maintaining a similar modulus, and the strain at break goes up to 1200% even after cross-linking. The tensile mechanical behavior is also compared in a stress–strain curve (Fig. 8). C1 and C2 series show similar slopes up to 600% strain, but a sudden increase in slope is observed for C2 series, especially C2-5, C2-10, and C2-15. Because the behavior of C2 series is similar to that of natural rubber, the four polymers, L-0, C1-10, C2-10, and natural rubber (NR), are plotted in Fig. 8(c). Notably, C2-10 is different from other PUs and is close to natural rubber in overall shape
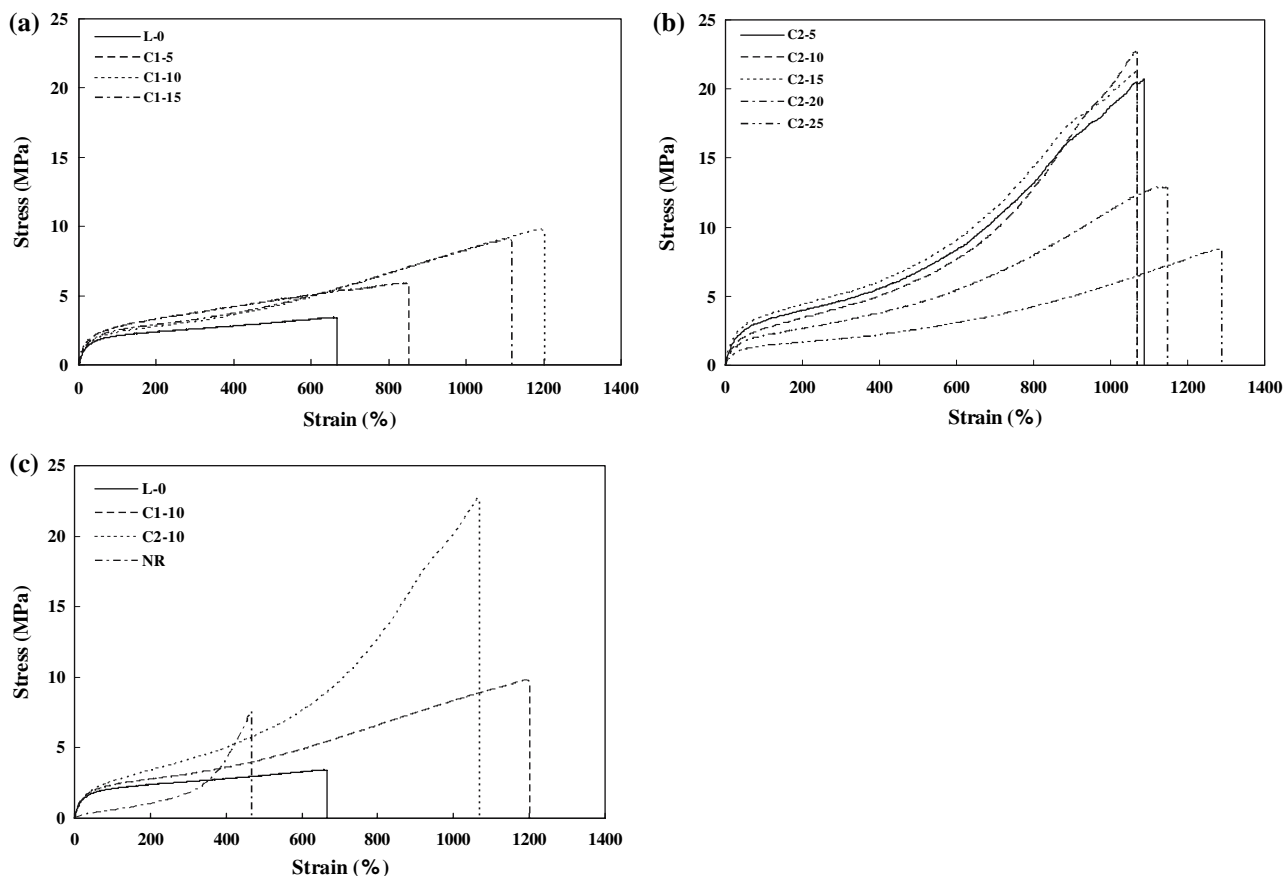
Fig. 8 Stress–strain curve of (**a**) C1 series, (**b**) C2 series, and (**c**) SMPU and natural rubber (NR)

except the higher stress and strain. The steep rise of stress in natural rubber originates from the strain-induced crystallization, and the same reasoning can be applied to the explanation of C2 series behavior. C2 series polymer aligns along the chain length because each polymer chain is connected by a PEG-200 spacer at its side and becomes stronger when stretched due to the strain-induced

crystallization. But C1 series, connected in a random manner, is unable to form the aligned structure and shows no sign of strain-induced crystallization. Previous experiments on SMPU have demonstrated that cross-linking of hard segment can increase maximum stress but strain is sacrificed instead. But the adoption of a flexible spacer and cross-linking at its side in C2 series elevates the
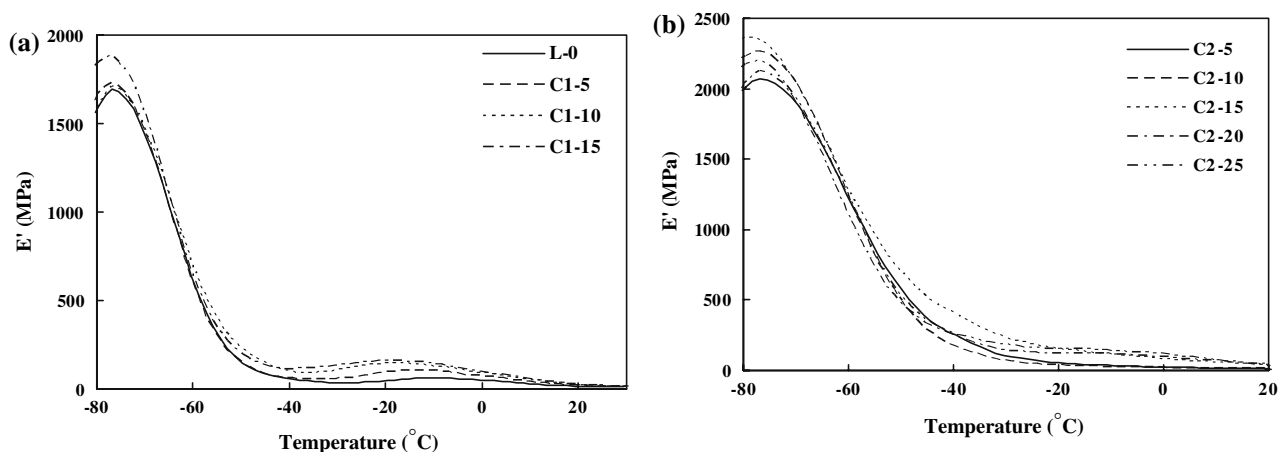

Fig. 9 Storage modulus vs. temperature profile of (**a**) L-0 and C1 series, and (**b**) C2 series
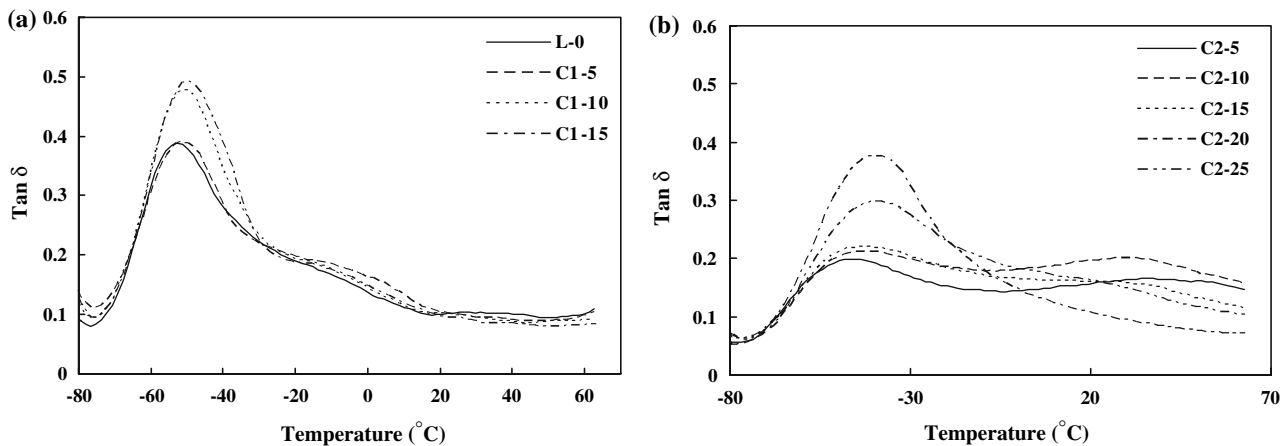
Fig. 10 Loss tangents vs. temperature profile of (**a**) L-0 and C1 series, and (**b**) C2 series

maximum stress without any sacrifice of strain. As noted in the above analyses and mechanical tests, C2 series is different and special because of the flexible spacer and sideway cross-linking.

Dynamic mechanical properties

Storage modulus (E′) and loss tangent (tan δ) results are shown in Figs. 9 and 10. It is already known that the cross-linked structure generally shows a higher storage modulus than the linear one. C2 series has a higher storage modulus than C1 series at the same glycerol content, which is due to the network structure of C2 series. The sudden decrease in storage modulus starting at –70 °C and ending at –20 °C is related to the phase transition of the soft segment. C2 series is lower in loss tangent, a measure of the resilience of

polymer, than C1 series, which is due to the high cross-link density of C2 series. T_g of the cross-linked SMPU in Table 4 is detected from the peak loss tangent value. As shown in shape memory effect section, the higher storage modulus of C2 series than that of C1 series results in the better shape recovery of C2 series over C1 series, but shape retention of C2 series compared to C1 series is sacrificed due to the higher storage modulus.

Shape memory effect

Cyclic shape memory test is used to compare the shape recovery rate and shape retention rate for the $T_m \pm 20$°C range (Figs. 11, 12). Shape memory test is generally carried out around T_g of soft segment for most of the thermally-induced shape memory polymers. In some cases, if T_g is too low, T_m of soft segment is used instead of T_g;

Fig. 11 Cyclic shape memory test of (**a**) L-0, (**b**) C1-5, (**c**) C1-10, and (**d**) C1-15
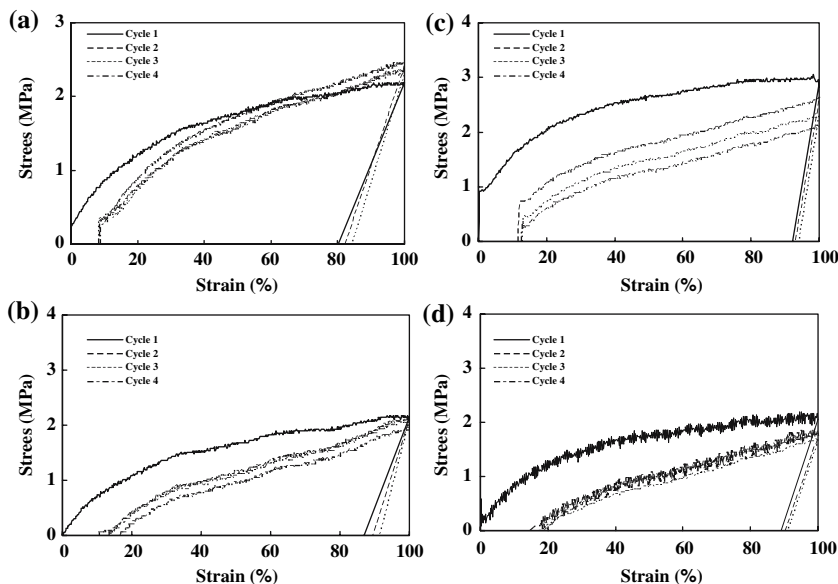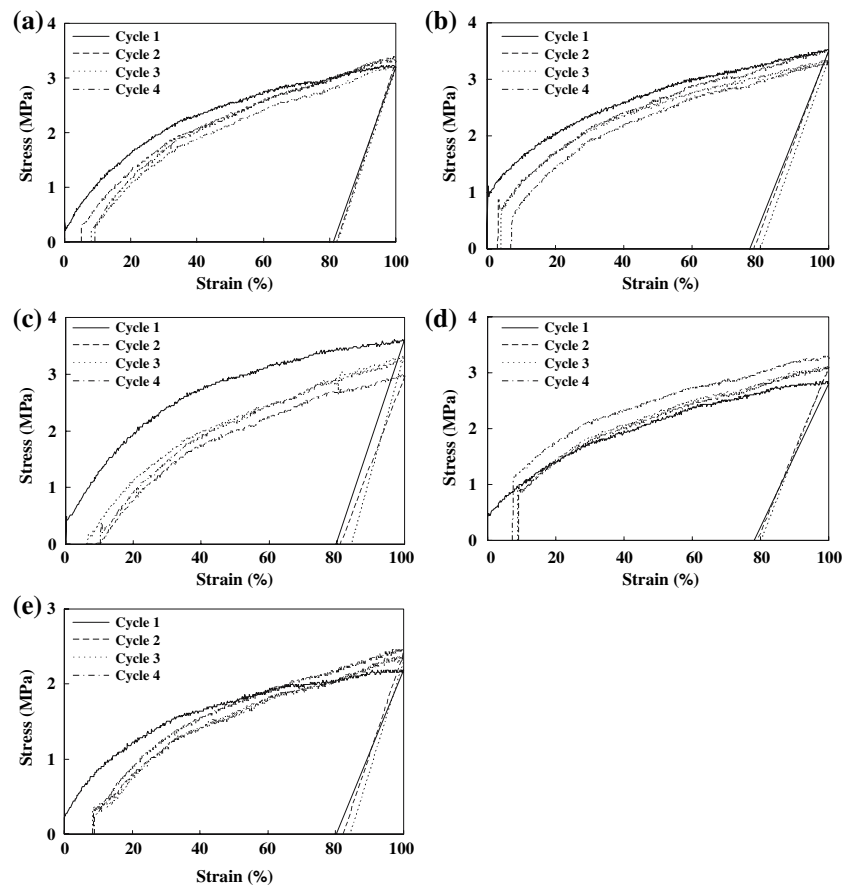
Fig. 12 Cyclic shape memory test of (**a**) C2-5, (**b**) C2-10, (**c**) C2-15, (**d**) C2-20, and (**e**) C2-25

such type of shape memory polymer is called T_m-type-shape memory polymer to differentiate it from T_g-type one. This SMPU belongs to T_m-type, because T_g is too low and it is hard to control the temperature around T_g [2, 12, 13]. As compared in Table 5, shape recovery process is over in 900 s at T_m + 20 °C. Shape recovery rate increases from 83.7% for L-0 to 89.3% for C1-5 and 96.8% for C2-10. C2 series exhibits a higher shape recovery rate than C1 series at the same glycerol content: 89.3% for C1-5 vs. 94.8% for C2-5, and 85.1% for C1-15 vs. 94.0% for C2-15 (Table 5). The shape recovery rate of C2-10, the best one of C2 series, does not fall below 93% even after cycle 4. Although many shape memory polymers, either polyester or polyurethane, have been tested by us, shape recovery rate is usually less than 95% and decreases to below 90% after cycle 3. Because the shape recovering force of C2 series is so strong, shape retention rate decreases compared to C1 series (Fig. 13). Shape recovery pictures of L-0, C1-10, and C2-10 are shown in Fig. 14. After each specimen is rolled, the time required for unfolding is compared. C1-10 reduces the unfolding time from 200 second of L-0 to 121 second, and C2-10 achieves the unfolding in just 66 second. Therefore, C2-10 recovers the original shape in one third of the time necessary for L-0. Along with all the above

analytical and mechanical results, the shape memory test also demonstrates that the alignment of polymer chains and the cross-linking at the side with a flexible spacer play a decisive role in improving the overall properties compared to the randomly cross-linked C1 series and linear L-0. Therefore, the finding of C2 series is very encouraging and argues the importance of polymer chain alignment and cross-linking method. More variations of SMPU based on C2 series can be produced in near future.

Table 5 Comparison of shape recovery speed of SMPU

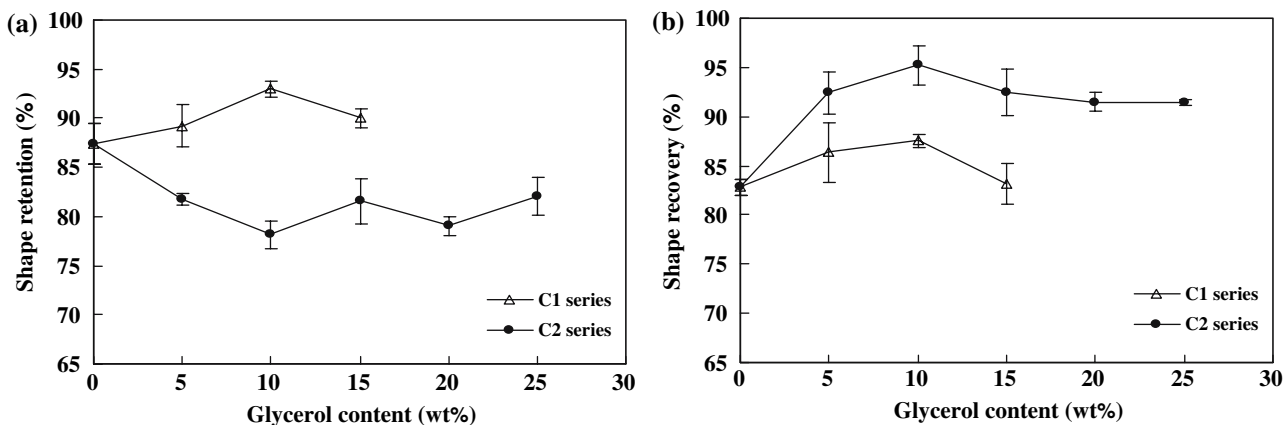| Sample code	Shape recovery rate (%)		
	300 s	600 s	Maximum
L-0	80.2	83.1	83.7
C1-5	80.0	82.7	89.3
C1-10	81.0	85.8	88.7
C1-15	80.4	82.3	85.1
C2-5	88.8	90.5	94.8
C2-10	90.7	93.7	96.8
C2-15	91.2	92.5	94.0
C2-20	88.0	90.8	90.8
C2-25	89.9	91.3	91.5

Fig. 13 (**a**) Shape retention and (**b**) shape recovery vs. glycerol content profile of SMPU

Conclusion

C2 series cross-linked with a PEG-200 spacer is compared with the linear L-0 and the randomly cross-linked C1 series. The cross-link density increases and the phase separation decreases with the increase of glycerol content for both C1 and C2 series. The ordered structure of hard segment is disrupted by cross-linking based on XRD analysis. The cross-linking of PU raises T_g and T_m for both C1 and C2 series. Maximum stress of C2 series increases up to 800% compared to L-0, while maintaining a similar strain.

The behavior of C2-10 in stress–strain curve is very similar to natural rubber, but both stress and strain are 300% higher than natural rubber. Shape recovery rate of C2-10 goes up to an amazing 96.8% and does not decrease below 93% after cycle 4, all without showing any drop in the shape recovery speed. All of the special and outstanding shape memory and mechanical properties of the C2 series originate from the parallel networking of the PU chains with the flexible PEG-200 spacer, and there remains much work to be done to attain the goal of a higher shape recovery rate and an upkeep of the high shape recovery rate after use.
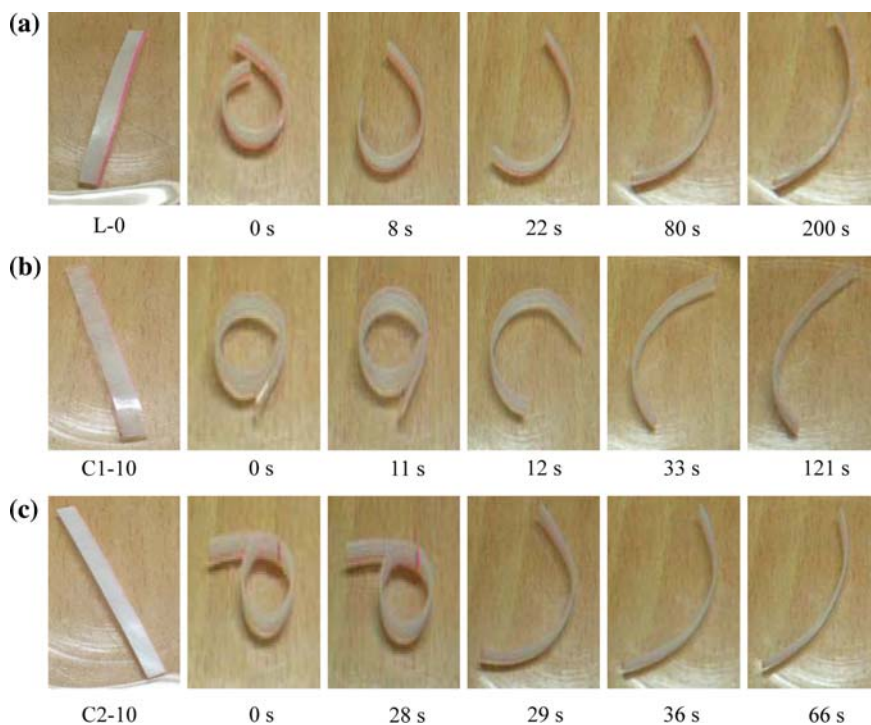

Fig. 14 Photographic comparison of shape recovery speed of (**a**) L-0, (**b**) C1-10, and C2-10

References

1. Yang JH, Chun BC, Chung YC, Cho JH (2003) Polymer 44:3251
2. Li F, Chen Y, Zhu W, Zhang X, Xu M (1998) Polymer 39:6929
3. Liang C, Rogers CA, Malafeew E (1997) J Intell Mater Syst Struct 8:380
4. Chun BC, Cha SH, Chung YC, Cho JW (2002) J Appl Polym Sci 83:27
5. Kim BK, Lee SY, Xu M (1996) Polymer 37:5781
6. Tobushi H, Hara H, Yamada E, Hayashi S (1996) Smart Mater Struct 5:483
7. Takahashi T, Hayashi N, Hayashi S (1996) J Appl Polym Sci 60:1061
8. Lee BS, Chun BC, Chung YC, Sul KI, Cho JW (2001) Macromolecules 34:6431
9. Ota S (1981) Radia Phys Chem 18:81
10. Chen LW, Lin JR (1998) J Appl Polym Sci 69:1563
11. Chen LW, Lin JR (1998) J Appl Polym Sci 69:1575
12. Hu J, Yang Z, Yeung L, Ji F, Liu Y (2005) Polym Int 54:854
13. Yang Z, Hu J, Liu Y, Yeung L (2006) Mater Chem Phys 98:368
14. Carey MA, Wellons SL, Elder DK (1984) J Cellular Plastic 20:42
15. Petrovic ZS, Javni I, Divjakovic V (1998) J Polym Sci B: Polym Phys 36:221
16. Hur MK, Kwak JM, Hur T (1996) Polymer (Korea) 20:392
17. Coleman MM, Lee KH, Skrovanek DJ, Painter PC (1986) Macromolecules 19:2149
18. Seymour RW, Estes GM, Cooper SL (1970) Macromolecules 3:579